

Soot formation in shock-tube pyrolysis of toluene–*n*-heptane and toluene–iso-octane mixtures

A. Alexiou and A. Williams

Department of Fuel and Energy, University of Leeds, Leeds LS2 9JT, UK
(Received 30 March 1994)

Soot formation during the pyrolysis of argon-diluted mixtures of toluene and *n*-heptane and of toluene and iso-octane in a reflected-shock tube was studied. Soot induction times and rates of formation measured at 632.8 nm by laser beam attenuation showed an Arrhenius dependence on reflected-shock temperature. The maximum in bell-shaped distribution of soot yield and concentration as a function of temperature decreased with increasing amount of *n*-heptane or iso-octane substituted for toluene. A kinetic model was used to explain the experimental trends and gave reasonable prediction of the experimental observations. The reduction in soot yield and concentration was attributed to the faster decomposition of the alkanes as well as to their decomposition products, which diverted the soot formation process from the more effective path of toluene pyrolysis to a slower route.

(Keywords: soot formation; pyrolysis; toluene–alkane mixtures)

The current move from leaded to unleaded gasoline has tended to increase the aromatics content of the fuel. Similar increases in aromatic constituents have occurred or are contemplated in both diesel and gas turbine fuels. This widespread increase in aromatics content has created a potential problem, in that more extensive pyrolysis of hydrocarbons takes place in combustion chambers, leading to in-chamber soot formation (and wall deposits) which may lead to smoke emission unless this soot is subsequently oxidized before emission.

There is now considerable experimental evidence to show that soot formation is related to the type of fuel burned, the type of flame (diffusion or premixed) and the flame temperature. It is now clear that soot formation in practical flames proceeds mainly through PAH formation; this explains the difference between the sooting tendency of aromatic and non-aromatic fuels, the former giving greater amounts of PAH and therefore more soot than the latter.

Early studies on *n*-heptane and iso-octane (2,2,4-trimethylpentane) include those of Orr¹, who also studied the combustion of C₂H₂, C₂H₄ and C₆H₆, and of Coats and Williams², who studied the ignition of *n*-C₇H₁₆. These authors showed that both *n*-C₇H₁₆ and iso-C₈H₁₈ exhibit extensive preflame activity leading to ethyne formation and subsequently soot formation. Although many experimental and modelling studies^{3–7} have been devoted to the combustion process, particularly in relation to engine knock, there have been relatively few studies of soot formation from the pyrolysis of these fuels. Soot formation from aromatic species, particularly toluene, has been extensively studied⁸. Under shock-tube conditions, only a few studies have been made of binary hydrocarbon mixtures^{9–11}. The only previous attempt to

study the pyrolysis of toluene–*n*-heptane mixtures is that of Simmons and Williams¹¹, who concluded that the rate of soot formation was significantly reduced when the amount of *n*-heptane in the mixture was increased.

In the present work, soot formation from toluene–*n*-heptane and toluene–iso-octane mixtures has been studied to obtain information about the effects of substituting aromatic for aliphatic fuels. Under the shock-tube conditions used, it is difficult to observe soot from *n*-heptane and iso-octane alone, so mixtures containing 30–70% toluene have been studied. A kinetic model describing the initial fuel pyrolysis, PAH growth and soot particle inception and growth has been used to interpret the results.

EXPERIMENTAL

The experiments were performed in a stainless steel reflected-shock tube² of diameter 73.7 mm, with driver and test sections 2.44 and 3.35 m long respectively. The observation windows were situated 12.5 mm from the end plate. The liquid fuels were purified by repeated freezing and evacuation. The test gas mixtures were prepared manometrically. The experimental conditions are summarized in Table 1. Incident-shock velocities were measured with five piezoelectric detectors. Reflected-shock conditions were calculated by the method of Gardiner *et al.*¹². The soot conversion, *Y*, was determined by measurement of the attenuation of the beam from a 15 mW He–Ne laser at 632.8 nm, and calculation by the formula of Graham *et al.*¹³:

$$Y \equiv \frac{[C]_{\text{soot}}}{[C]_{\text{total}}} = \frac{N_A \rho \lambda}{72 \pi E_{(m)} l [C]_{\text{total}}} \ln \frac{I_0}{I} \quad (1)$$

Table 1 Experimental conditions behind reflected shock waves

Mixture (mol% in Ar)			<i>T</i> (K)	<i>P</i> (kPa)	C atom concentration (10 ¹⁷ cm ⁻³)
C ₇ H ₈	<i>n</i> -C ₇ H ₁₆	iso-C ₈ H ₁₈			
0.5	—	—	1826–2233	195–262	2.707–2.97
1.0	—	—	1668–2414	187–329	5.68–6.9
1.5	—	—	1566–2345	185–351	8.98–11.5
0.9	0.1	—	1667–2143	189–278	5.739–6.57
0.7	0.3	—	1733–2419	205–340	5.99–7.12
0.5	0.5	—	1754–2361	218–334	6.14–7.168
0.3	0.7	—	1824–2384	231–346	6.41–7.35
0.7	—	0.3	1634–2418	189–337	6.11–7.48
0.5	—	0.5	1740–2380	215–347	6.7–7.915
0.3	—	0.7	1794–2399	232–362	7.208–8.41

where $[C]_{\text{soot}}$ is the concentration of carbon atoms in the soot particles formed, $[C]_{\text{total}}$ is the initial concentration of carbon atoms in the fuel, N_A is the Avogadro constant, ρ is the density, λ is the wavelength, l is the length of the optical path, which in the present shock tube is 0.0737 m, I_0 and I are the intensities of the incident and transmitted light respectively, and $E_{(m)}$ is a function of the complex refractive index, m :

$$E_{(m)} = -\text{Im} \left[\frac{m^2 - 1}{m^2 + 2} \right] = \frac{6nk}{(n^2 - k^2 + 2)^2 + 4n^2k^2} \quad (2)$$

where $\text{Im}[\]$ is the imaginary part of $[\]$, and n and k are the real and imaginary parts of the complex refractive index respectively.

The 'soot yield', meaning the fractional conversion of the carbon atoms in a hydrocarbon fuel to soot, and 'soot concentration', meaning the absolute amount of carbon atoms per cm³ accumulated in soot, were used as practical measures of soot formation. These measures provide essentially identical information, but it is useful to use both to distinguish the sooting tendencies in binary hydrocarbon mixtures⁹. The value of $E_{(m)}$ chosen was that of Charalampopoulos and Chang¹⁴, 0.253 at wavelength 632.8 nm.

RESULTS AND DISCUSSION

A soot induction period, τ_{soot} , defined as the time interval between the reflected pressure signal and the onset of attenuation (1% signal rise), ranging from 20 to 2100 μs was observed before any absorption occurred. Correlation equations in the form of global rate expressions for delay time were obtained for the pyrolysis of toluene, toluene-*n*-heptane and toluene-iso-octane diluted in argon, within the range of experimental conditions in Table 1, as follows:

$$\tau_{\text{soot}} = 8.42 \times 10^{-12} \exp\left(\frac{21\,770}{T}\right) [C_7H_8]^{-1.57} \quad (3)$$

$$\tau_{\text{soot}} = 2.53 \times 10^{-11} \exp\left(\frac{24\,056}{T}\right) [C_7H_8]^{-1.43} \times [n\text{-}C_7H_{16}]^{0.359} \quad (4)$$

$$\tau_{\text{soot}} = 1.87 \times 10^{-11} \exp\left(\frac{28\,145}{T}\right) [C_7H_8]^{-0.925} \times [\text{iso-}C_8H_{18}]^{0.349} \quad (5)$$

where τ_{soot} is the induction time for soot appearance (s),

T is the reflected-shock temperature (K), and the initial post-shock concentrations of the fuel mixtures are in mol m⁻³. The measured induction times for soot appearance showed an Arrhenius dependence on the reflected-shock temperature (T). The inverse dependence of the induction time on toluene concentration indicates that soot forms earlier as the partial pressure of toluene increases.

The maximum rate of soot formation determined from the maximum slope on the oscillogram was observed to vary with temperature and concentration of the hydrocarbons. Correlation equations for the rate of soot formation for toluene, toluene-*n*-heptane and toluene-iso-octane diluted in argon were determined within the range of experimental conditions given in Table 1, as follows:

$$R_{\text{soot}} = 6.5 \times 10^6 \exp\left(\frac{-10\,224}{T}\right) [C_7H_8]^{1.32} [Ar]^{0.194} \quad (6)$$

$$R_{\text{soot}} = 2.2 \times 10^6 \exp\left(\frac{-13\,712}{T}\right) [C_7H_8]^{0.902} \times [n\text{-}C_7H_{16}]^{-0.383} \quad (7)$$

$$R_{\text{soot}} = 3.2 \times 10^6 \exp\left(\frac{-15\,756}{T}\right) [C_7H_8]^{0.832} \times [\text{iso-}C_8H_{18}]^{-0.466} \quad (8)$$

where R_{soot} is the rate of soot formation in mol m⁻³ s⁻¹. The rates of soot formation also showed an Arrhenius dependence on the reflected-shock temperature (T). A positive power dependence on fuel concentration indicates that an increase in concentration tends to increase the rate of soot formation. From these equations it can be seen that soot induction time and rate of soot formation follow similar trends. It was also observed that while the induction time decreased to a minimum with increasing temperature, the rate of soot formation passed through a maximum. This emphasizes a similarity between soot initiation, precursor formation and particle inception. Both *n*-heptane and iso-octane increased the induction time and reduced the rate of soot formation from toluene.

Although Equations (3)–(8) adequately describe the results for mixtures of *n*-heptane and iso-octane with toluene, they are not applicable outside the range of the experimental conditions or compositions studied here. To apply these results to practical (commercial) fuels which contain aromatic and aliphatic fractions, it can be assumed that the toluene is equivalent to the former and *n*-heptane to the latter. Thus the influence of the aliphatic component on soot formation can be estimated. The following approximate expression was derived to apply these results to practical fuels:

$$R_{\text{soot}} = F[H]^{1.32} [Ar]^{0.194} \exp\left(\frac{-10\,224}{T}\right) \quad (9)$$

where F is a factor depending on the toluene/*n*-heptane and toluene/iso-octane ratios, and $[H]$ is the concentration of total hydrocarbons. Figure 1 shows values of F at 1800 K. The effects of methanol, ethanol and oxygen addition to the toluene are also shown. Very similar sharp reductions in soot formation are achieved

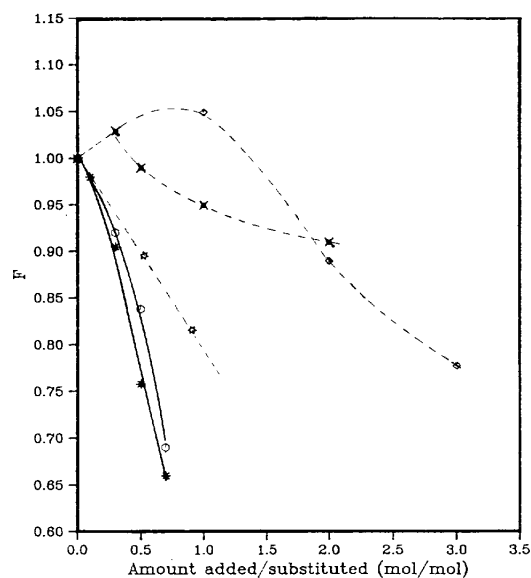


Figure 1 Factor F as a function of amount of fuel added to toluene, at 1800 K. Solid lines: n -heptane (*); iso-octane (O). Dashed lines: oxygen (☆); methanol (★); ethanol (◇)

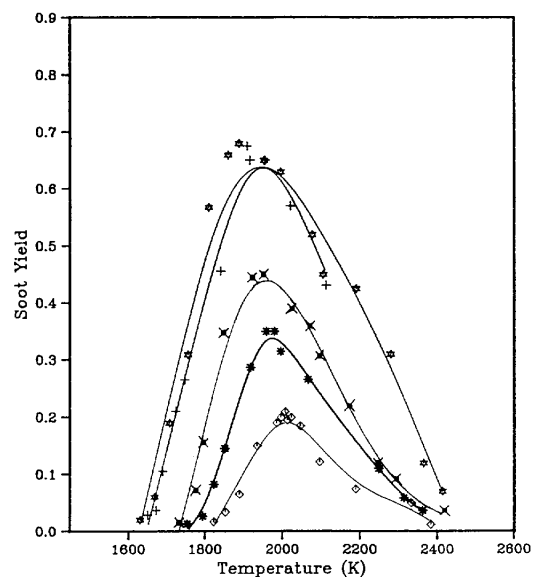


Figure 2 Soot yield from pyrolysis of toluene- n -heptane mixtures of total concentration 1.0 mol% in Ar. n -Heptane concentration (mol%): ☆, 0.0; +, 0.1; ★, 0.3; *, 0.5; ◇, 0.7

by increasing the amount of n -heptane and iso-octane substituted for toluene.

The sooting behaviour of toluene- n -heptane mixtures is shown in Figures 2 and 3. Soot formation is reduced by increasing the amount of n -heptane in the fuel mixture. A shift in maximum soot yield and concentration to higher temperatures is also observed. Very similar results were obtained when iso-octane was substituted for toluene, as shown in Figures 4 and 5. This remarkable

similarity of behaviour of the two types of mixture indicates the role of the initial fuel decomposition in the soot formation process as discussed below.

The concept of a global rate expression to describe phenomena such as induction times and rates of soot formation arises from the complexity of the chemical reactions concerned. However, is very difficult to compare the current correlation equations with others in the

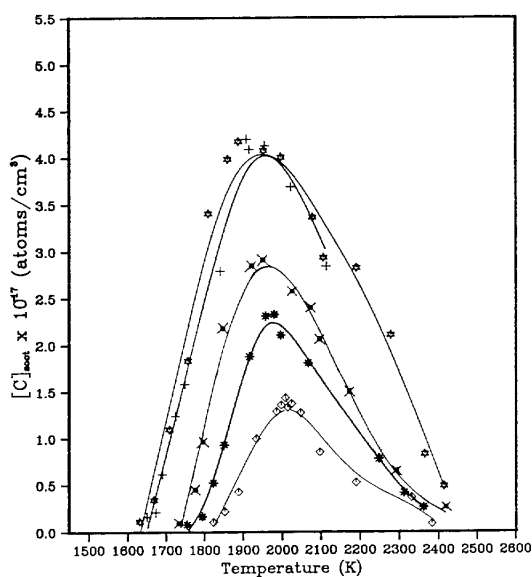


Figure 3 Soot concentration from pyrolysis of toluene- n -heptane mixtures. Concentrations as in Figure 2

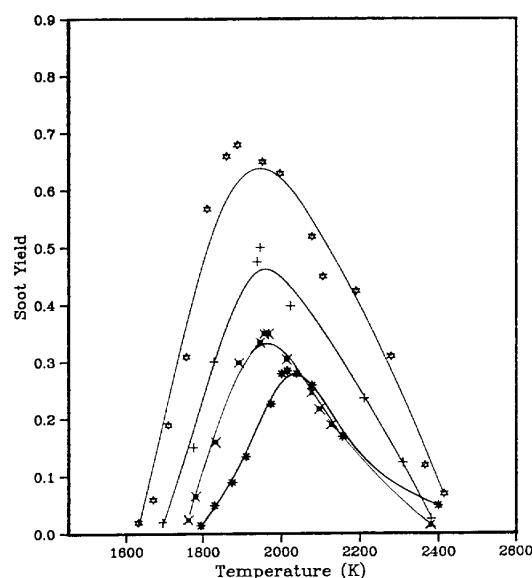


Figure 4 Soot yield from pyrolysis of toluene-iso-octane mixtures of total concentration 1.0 mol% in Ar. Iso-octane concentration (mol%): ☆, 0.0; +, 0.3; ★, 0.5; *, 0.7

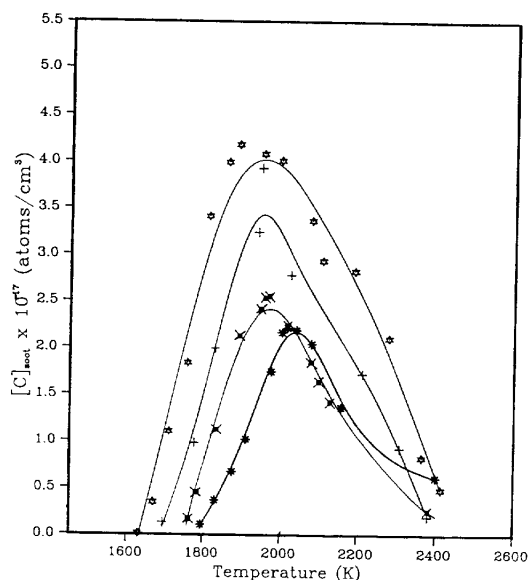


Figure 5 Soot concentration from pyrolysis of toluene-iso-octane mixtures. Concentrations as in Figure 4

literature^{11,15}, since the sensitivity of the detection system, the interpretation of the experimental signals and the design of the shock tube could affect the final result and thus the equations obtained. Furthermore, the accuracy of the various equations in the literature should be tested by comparison with experimental data on soot concentrations measured in conjunction with local concentrations of hydrocarbons and oxygen. However, comparison of the soot yield and amount during toluene pyrolysis with other optical data^{8,13,15} produces a broad agreement. As mentioned previously^{8,10,15}, the soot yield and amount are not universally constant but depend on experimental variables such as observation time, total pressure, initial hydrocarbon concentration and the wavelength used in the measurements. In the present work the maximum soot yield and amount were measured irrespective of the observation time. During toluene pyrolysis it was found that the maximum occurred at a reaction time > 1 ms and that soot yield and amount passed through a maximum at ~ 1950 K.

KINETIC MODELLING

An understanding of all the chemical processes taking place during soot formation can be achieved only by kinetic modelling. However, the accurate prediction of soot formation is still a formidable problem, because of the uncertainties about the factors governing the pyrolysis and oxidation reactions, in particular those concerning the aromatic compounds, which are very important in soot formation, as well as the lack of reliable thermochemical data^{9,16}. Detailed models describing the formation of large PAH molecules and soot have been proposed for shock-tube conditions^{9,16,17} and applied in a limited sense also to flames^{18,19}. The role of PAH dimerization and the probable initiation of soot particle growth from PAH under shock-tube conditions, in

addition to the growth of soot from C_2H_2 and other species, was not considered^{9,16,17}. On the other hand, simplified mechanisms have also been suggested for flame conditions, for example by Leung *et al.*²⁰. However, their mechanism is open to debate, since the importance of the aromatics and large PAH was not taken into account.

The current model describing soot formation consists of three stages¹⁸: (1) a detailed description of pyrolysis of the parent fuel and initial formation of small PAH species; (2) growth of the PAH; and (3) soot particle inception and growth.

The mechanism of soot formation is generally assumed to involve the decomposition of the parent hydrocarbon fuel to give ethyne, the formation of benzene from ethyne, and further reactions to form increasingly large PAH molecules which are the soot precursors. The rate of formation of the first ring determines the rate of PAH formation, soot inception and soot mass growth²¹. In the case of aromatics there is always at least one ring already present and therefore the initial ring formation is bypassed. From non-aromatic fuels the first ring has to be formed, and two mechanisms have been put forward. One involves C_2H_3 addition to C_2H_2 . At high temperatures this forms C_4H_4 and is followed by C_2H_2 addition to an $n-C_4H_3$ radical formed by H atom abstraction from the C_4H_4 . At lower temperatures the addition of C_2H_2 to C_2H_3 results in $n-C_4H_5$, which upon addition of C_2H_2 produces C_6H_6 ¹⁸. In the other mechanism, suggested by Miller and Melius²², C_6H_6 is formed by combination of C_3H_3 radicals. In the present model, both schemes were used.

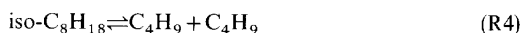
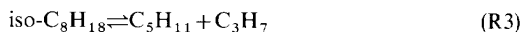
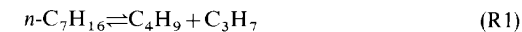
The second part of the model describing PAH growth is that proposed by Frenklach *et al.*⁹. This part of the mechanism is based on ethyne addition to an aromatic molecule and reactivation of the resulting aromatic species by hydrogen abstraction. In the third part of the model, all the large PAH formed during the second stage are assumed to collide and form dimers, the dimers further colliding with other monomers or dimers to form trimers, etc.¹⁸. Such a combination of PAH reactions results in particle inception. These reactions are treated as irreversible¹⁸. A minimum size of 1 nm is assumed²⁰. The growth of the incipient particle is based on the model described by Harris and Weiner²³ and is given by

$$\frac{dM}{dt} = kS[C_2H_2] \quad (10)$$

where M is the total soot concentration in $g\ cm^{-3}$, S is the surface area in $cm^2\ cm^{-3}$, and k is the rate constant for the reaction which converts ethyne into soot, which in the present work is taken as $5 \times 10^{-3}\ g\ cm^{-2}\ s^{-1}\ atm^{-1}$, for a reaction time of 1 ms²³. Owing to the scarcity of experimental data on the growth of the incipient particle from different species, the same value of k is used for growth from C_4H_2 and C_6H_6 . The contribution from C_4H_2 and C_6H_6 as well as from larger hydrocarbon species was found to be small. However, the dimerization of PAH plays an indirect role in soot growth by initially supplying the surface area for growth. The larger the molecule taking part in the dimerization process, the larger the incipient particle formed and thus the larger the surface area for subsequent growth, mainly from ethyne.

The unimolecular decomposition of *n*-heptane and

iso-octane involves the following reactions⁴⁻⁷:



As can be seen, both fuels decompose to similar species, such as C_5H_{11} , C_4H_9 and C_3H_7 , and eventually into C_2H_2 through C_2H_4 and/or C_2H_5 . These species interfere with the mechanism of soot formation from toluene, resulting in a reduction in soot yield. Selected species concentrations as a function of reaction time are plotted in Figures 6 and 7 for 0.7 mol% C_7H_8 + 0.3 mol% $n\text{-C}_7\text{H}_{16}$ at 1805 K and for 0.7 mol% C_7H_8 + 0.3 mol% iso- C_8H_{18} at 1795 K respectively. The nomenclature of the aromatic species featured in these graphs is that of ref. 16; e.g. A5 represents a PAH molecule containing five rings. C_{nucl} is the incipient particle after the dimerization of the PAH and before the growth process. Both $n\text{-C}_7\text{H}_{16}$ and iso- C_8H_{18} decompose more rapidly than C_7H_8 . This effect, in addition to the decomposition species, diverts soot formation from the more effective path provided by the presence of the first ring and biphenyl formation (condensation reactions) to a slower one in which the first step must involve the formation of

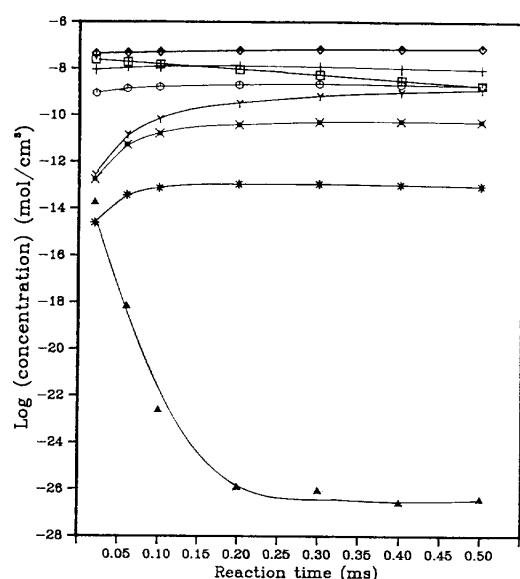


Figure 6 Computed species concentrations as a function of reaction time for a 0.7 mol% toluene-0.3 mol% n -heptane mixture at 1805 K. \square , Toluene; \blacktriangle , n -heptane; +, benzene; \diamond , ethyne; \circ , A5; \star , A11; $*$, C_{nucl} ; Y, soot

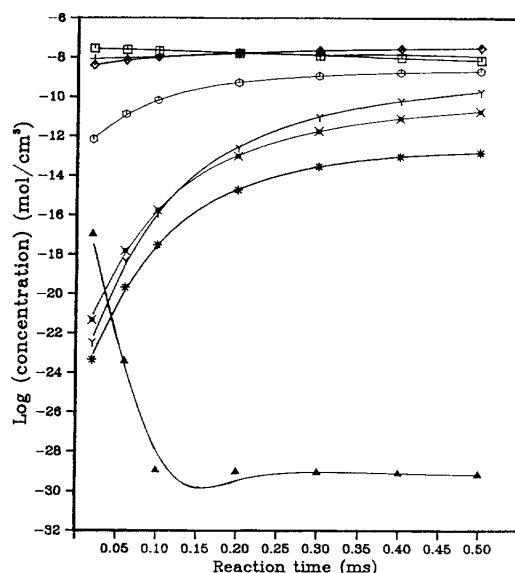


Figure 7 Computed species concentrations as a function of reaction time for a 0.7 mol% toluene-0.3 mol% iso-octane mixture at 1795 K. Symbols as in Figure 6, except \blacktriangle , iso-octane

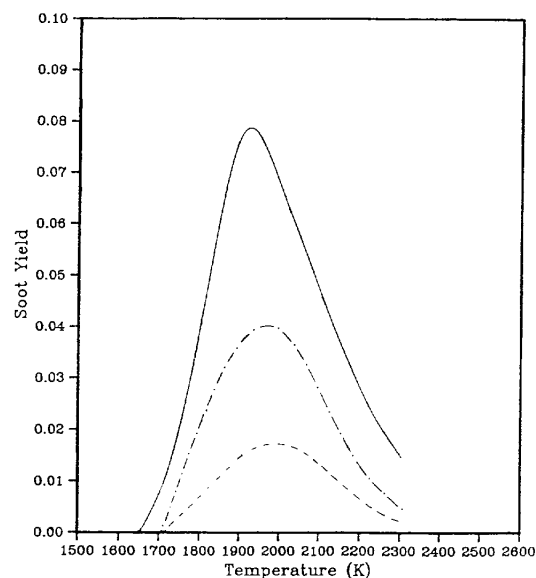


Figure 8 Comparison of computed soot yields from pyrolysis of toluene and toluene- n -heptane mixtures at 0.5 ms reaction time. Total concentration 1.0 mol% in Ar. n -Heptane concentration (mol%): —, 0.0; ---, 0.3; ···, 0.7

the first ring. The delay in forming the first ring and subsequently higher PAH is therefore responsible for the lower conversion of these particular fuels to soot as well as for the shift in the bell-shaped distribution to higher temperatures, as seen in Figures 8 and 9, showing the computed soot yields for the two types of alkane-toluene mixture. The sooting behaviour of both fuels is that expected from a typical aliphatic fuel.

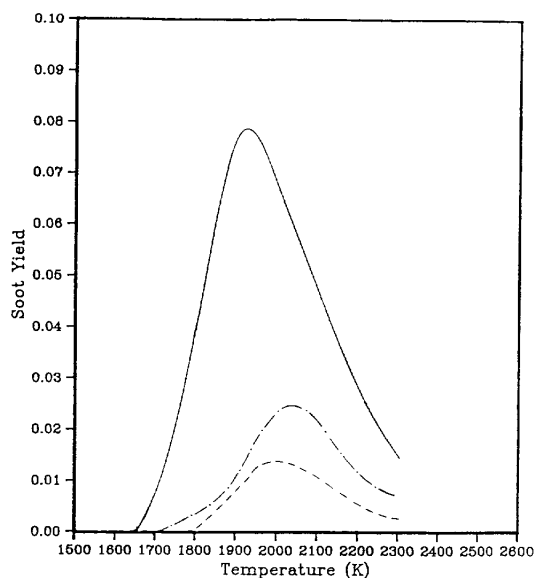


Figure 9 Comparison of computed soot yields from pyrolysis of toluene and toluene-iso-octane mixtures. Concentrations of mixture and alkane as in Figure 8

CONCLUSIONS

1. The soot induction times and the rates of soot formation as measured by laser beam attenuation during pyrolysis of toluene and in toluene-*n*-heptane and toluene-iso-octane mixtures show an Arrhenius dependence on the reflected-shock temperature. The correlation equations describing induction times and rates of soot formation indicate that *n*-heptane and iso-octane substitution for toluene increases the induction time and reduces the rate of soot formation compared with those from toluene alone.
2. Soot yields and concentrations exhibit a bell-shaped distribution as a function of temperature. Partial replacement of toluene by *n*-heptane and by iso-octane results in a reduction in soot yield and concentration compared with those from toluene alone. This reduction also results in a shift in maximum soot yield to higher temperatures. The very similar distribution of soot yield and concentration for both types of alkane-toluene mixture indicates a similar soot formation process.
3. The computational results reasonably predict the experimental trends. A reduction in soot yield as a

result of *n*-heptane and iso-octane addition to toluene is obtained. This is due to the faster decomposition of *n*-heptane and iso-octane as well as to their decomposition products. The similar sooting behaviour of both fuel mixtures is attributed to the same products of thermal decomposition of the alkanes, which must interfere with the sooting mechanism of toluene.

REFERENCES

- 1 Orr, C. R. In 'Ninth Symposium (International) on Combustion', The Combustion Institute, Pittsburgh, 1963, p. 1034
- 2 Coats, C. M. and Williams, A. In 'Seventeenth Symposium (International) on Combustion', The Combustion Institute, Pittsburgh, 1979, p. 611
- 3 Dryer, F. L. and Brezinsky, K. *Combust. Sci. Technol.* 1986, **45**, 199
- 4 Westbrook, C. K. and Pitz, W. K. In 'Complex Chemical Reaction Systems' (Eds J. Warnatz and W. Jäger), Springer-Verlag, Berlin, 1987
- 5 Westbrook, C. K., Warnatz, J. and Pitz, W. J. In 'Twenty-second Symposium (International) on Combustion', The Combustion Institute, Pittsburgh, 1988, p. 893
- 6 Warnatz, J. In 'Twentieth Symposium (International) on Combustion', The Combustion Institute, Pittsburgh, 1984, p. 845
- 7 Axelsson, E. I., Brezinsky, K., Pitz, W. J. and Westbrook, C. K. In 'Twenty-first Symposium (International) on Combustion', The Combustion Institute, Pittsburgh, 1986, p. 783
- 8 Frenklach, M., Taki, S. and Matula, R. A. *Combust. Flame* 1983, **49**, 275
- 9 Frenklach, M., Yuan, T. and Ramachandra, M. K. *Energy Fuels* 1988, **2**, 462
- 10 Alexiou, A. and Williams, A. *Fuel* (to be published)
- 11 Simmons, B. and Williams, A. *Combust. Flame* 1988, **71**, 219
- 12 Gardiner, W. C., Jr, Walker, B. F. and Wakefield, C. B. In 'Shock Waves in Chemistry' (Ed. A. Lifshitz), Dekker, New York, 1981, Ch. 7
- 13 Graham, S. C., Hommer, J. B. and Rosenfeld, J. L. D. *Proc. Roy. Soc. A* 1975, **344**, 259
- 14 Charalampopoulos, T. T. and Chang, H. *Combust. Sci. Technol.* 1988, **59**, 401
- 15 Wang, T. S., Matula, R. A. and Farmer, R. C. In 'Eighteenth Symposium (International) on Combustion', The Combustion Institute, Pittsburgh, 1981, p. 1149
- 16 Frenklach, M., Clary, D. W., Yuan, T., Gardiner, W. C., Jr and Stein, S. E. *Combust. Sci. Technol.* 1986, **50**, 79
- 17 Frenklach, M., Clary, D. W., Gardiner, W. C., Jr, William, C. and Stein, S. E. In 'Twentieth Symposium (International) on Combustion', The Combustion Institute, Pittsburgh, 1984, p. 887
- 18 Frenklach, M. and Wang, H. In 'Twenty-third Symposium (International) on Combustion', The Combustion Institute, Pittsburgh, 1990, p. 1559
- 19 Markatou, P., Wang, H. and Frenklach, M. *Combust. Flame* 1993, **93**, 467
- 20 Leung, K. M., Lindstedt, R. P. and Jones, W. P. *Combust. Flame* 1991, **87**, 289
- 21 Glassman, I. In 'Twenty-second Symposium (International) on Combustion', The Combustion Institute, Pittsburgh, 1988, p. 295
- 22 Miller, J. A. and Melius, C. F. *Combust. Flame* 1992, **91**, 21
- 23 Harris, S. J. and Weiner, A. M. *Combust. Sci. Technol.* 1983, **32**, 267